VILNIUS TECH
Vilnius Gediminas
Technical University

Numerical Study of the Shielding Properties of a Ferrofluid Taking into Account Magnetophoresis and Particle Interaction

Olga Lavrova[a] and Viktor Polevikov[b]

[a]*Faculty of Mechanics and Mathematics, Belarusian State University*

[b]*Faculty of Applied Mathematics and Informatics, Belarusian State University*

Independence Ave. 4, 220030 Minsk, Belarus

E-mail(*corresp.*): `lavrovaolga@mail.ru`

E-mail: `polevikov@bsu.by`

Abstract. Shielding properties of a cylindrical thick-walled ferrofluid layer that protects against externally applied uniform magnetic fields are numerically investigated. We take into account the diffusion of magnetic nanoparticles in the ferrofluid with magnetic dipole-dipole, steric and hydrodynamic interactions between particles. Permeability of the ferrofluid is considered to be dependent on the magnetic-field strength and the particle concentration. A combined method of finite differences and boundary elements is applied to solve a nonlinear transmission problem of magnetostatics in the whole space, augmented by nonlinear algebraic equations based on the mass transfer equation for magnetic nanoparticles in ferrofluids. Numerical experiments revealed that the diffusion of particles has negligible influence on the shielding properties at weak and strong intensities of the applied magnetic field when comparing with the results of computations for a uniform particle distribution.

Keywords: magnetostatics problem, diffusion problem, finite-difference method, boundary element method, Newton's method, ferrofluid, magnetic shielding.

AMS Subject Classification: 35K57; 35Q60; 65N06; 65N38.

1 Introduction

Shielding problems of electromagnetic fields have been actively studied for solid thin-walled layers, see, e.g., references in [9], whereas a ferrofluid, as a soft

magnetic material, could potentially be used in shielding applications. For example, conducting ferrofluid composites are investigated in [12] as a promising candidate for microwave shielding applications.

Other composites, based on textile materials with ferrofluid, with the purpose of shielding from the electromagnetic fields of a wide frequency range were developed and studied in [7]. Experimental measurements and analysis of the shielding effectiveness of a ferrofluid under radio frequency electromagnetic fields were performed in [5, 6]. Moreover, in patent [13] a magnetic field measurement system was suggested and described. In that system the ferrofluid is arranged to create magnetically shielded areas that contain the magnetometers of the measurement system to reduce or eliminate the ambient background magnetic field (e.g., the Earth's magnetic field) at the magnetometers. Magnetic shielding of an external uniform magnetic field by ferrofluids is numerically studied in the current research, based on various mathematical models.

Ferrofluids are stable colloidal suspensions of ferromagnetic nanoparticles in a nonmagnetic carrier-liquid [1, 2, 3, 20]. When no external magnetic field is applied, the ferroparticles of a diameter about 10 nm are in Brownian motion inside the carrier-liquid. Once affected by an externally applied magnetic field, the particle diffusion in the direction of field gradient, named as magnetophoresis, occurs inside the ferrofluid as well.

A traditional strategy for reducing quasi-static magnetic fields in a specific region consists of inserting a shield of an appropriate material, whose properties allow to decrease the magnetic field magnitude, emitted by the source, inside the specific region [4]. An infinite cylindrical shield, made of a thick ferrofluid layer, in an externally applied uniform magnetic field is investigated in the current research via numerical modelling.

Numerical investigations of magnetic shielding by a cylindrical thick-walled ferrofluid layer have their origins in [9, 15]. Mathematical models in [9, 15] were constructed on the basis of Maxwell's equations under the assumption that the magnetic particles inside the ferrofluid are uniformly distributed for any intensities of the externally applied field, thereby excluding the effects of magnetophoresis. The present study continues research in [9, 15] by taking into account the diffusion of nanosized ferroparticles (magnetophoresis) and particle interactions in the carrier-liquid, in order to estimate an influence of the steady-state particle redistribution on the degree of shielding.

Three mathematical models are constructed in which the magnetostatics equations in [9] and the diffusion equations are coupled with each other. Computations are made for three differently concentrated ferrofluids. These ferrofluids are described in [21, Table II], with the volume fraction of the magnetic phase equaled to 0.05, 0.1 and 0.16, respectively.

2   Mathematical model

The geometry for the problem under consideration is similar to the one in [9,15], see Figure 1. The two-dimensional geometry description is possible due to the assumptions that a cylindrical ferrofluid layer is infinitely long in the z-direction and that an applied magnetic field is uniform with the only non-zero component

$h_0 = const > 0$ in the y-direction, see Figure 1. Additionally, it results in a symmetry of the problem statement relative to the coordinate axes Ox and Oy of the Cartesian coordinate system Oxy. Therefore, the layer is described only by its cross-section Ω_2 at the positive quadrant of the Cartesian coordinate system Oxy, see Figure 1. The inner domain Ω_1, which defines the shielded region, and the outer domain Ω_3, which defines the region of the magnetic-field source, are filled with vacuum of the permeability $\mu_0 = 4\pi \cdot 10^{-7}$ H/m. Domains Ω_1 and Ω_3 are separated by the layer Ω_2 and have the common boundaries with the layer such as $\gamma_1 := \overline{\Omega}_1 \cap \overline{\Omega}_2$ and $\gamma_2 := \overline{\Omega}_2 \cap \overline{\Omega}_3$. Refer to Figure 1.
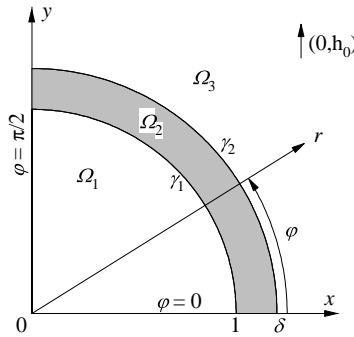
Figure 1. Two-dimensional geometry of the problem under consideration with an internal domain of a cylinder Ω_1 and an external domain Ω_3, corresponding to nonmagnetic media, and a domain Ω_2, filled with the ferrofluid.

Space variables x and y together with space variable r of the corresponding polar coordinate system $Or\varphi$, see Figure 1, are dimensionless over the inner radius of the cylindrical layer Ω_2. The dimensionless outer radius of the layer δ is considered as a parameter for the problem under consideration. Values of $\delta \in [1.01, 2]$ are used for computations. The magnetic field h is dimensionless over H_* for the problem under consideration, where $H_* = kT/(\mu_0 m)$, $k = 1.38 \cdot 10^{-23}$ J/K is Boltzmann's constant, T is the absolute temperature of the fluid, m is magnetic moment of a ferroparticle.

To investigate the magnetic shielding by weakly, moderately and highly concentrated ferrofluids, the mathematical models in the form of the Maxwells equations for different magnetization laws of ferrofluids are considered in [9] under an assumption of a uniform particle distribution inside the ferrofluid. These mathematical models, formulated in the polar coordinates (r, φ) in terms of magnetostatic potentials $u_i(r, \varphi) : \Omega_i \to \mathbb{R}$, $i = \overline{1,3}$, consist of the nonlinear Laplace-type equation in the ferrofluid domain

$$\frac{1}{r}\frac{\partial}{\partial r}\left(\mu(h_2)r\frac{\partial u_2}{\partial r}\right) + \frac{1}{r^2}\frac{\partial}{\partial \varphi}\left(\mu(h_2)\frac{\partial u_2}{\partial \varphi}\right) = 0 \quad \text{in } \Omega_2 \qquad (2.1)$$

with the intensity of the magnetic field $h_i := h_i(r, \varphi) : \Omega_i \to \mathbb{R}$, $i = \overline{1,3}$, where $h_i(r, \varphi) = \left(\left(\frac{\partial u_i}{\partial r}\right)^2 + \left(\frac{1}{r}\frac{\partial u_i}{\partial \varphi}\right)^2\right)^{1/2}$. The relative magnetic permeability of the

ferrofluid $\mu(h)$ is defined by following three distinct formulations:

$$\mu_{(1)}(h) = 1 + 3\chi_L L(h)/h, \tag{2.2}$$

$$\mu_{(2)}(h) = 1 + 3\chi_L L\left(h_{(2)}\right)/h, \quad h_{(2)} = h + \chi_L L(h), \tag{2.3}$$

$$\mu_{(3)}(h) = 1 + 3\chi_L \frac{L\left(h_{(3)}\right)}{h}, \quad h_{(3)} = h + \chi_L L(h) + \frac{\chi_L^2}{16} L(h) \frac{dL(h)}{dh}. \tag{2.4}$$

Each of them describes weakly, moderately and highly concentrated ferrofluids, respectively. Refer to [9] for details. Here, $\chi_L = M_s/(3H_*)$ is the Langevin susceptibility, M_s saturation magnetization of the ferrofluid. The function $L(h) = \coth(h) - 1/h$ is the Langevin function, and the magnetic field intensity h, dimensionless over H_*, as the argument of the Langevin function, is also named as the Langevin parameter, see e.g. [20]. $h_{(2)}$ and $h_{(3)}$ denote the effective fields, corresponding to the magnetization laws, suggested in [19] and [8] for moderately and highly concentrated ferrofluids, respectively. The Equation (2.1) in the layer is coupled with the boundary integral equation on the inner boundary γ_1 of the layer, see [9] for details,

$$\int_0^{\pi/2} q_1(\varphi) \left[u^*\left(\xi_0, \xi_1^{[1]}\right) + u^*\left(\xi_0, \xi_2^{[1]}\right) - u^*\left(\xi_0, \xi_3^{[1]}\right) - u^*\left(\xi_0, \xi_4^{[1]}\right) \right] d\varphi$$
$$= \pi u_1(\xi_0) \quad \text{for } \xi_0 \in \gamma_1, \tag{2.5}$$

where $q_1(\varphi) := \frac{\partial u_1}{\partial r}(1, \varphi)$. Equation (2.1) is also coupled with the boundary integral equation on the outer boundary γ_2 of the layer, see [9] for details,

$$\int_0^{\pi/2} q_3(\varphi) \left[u^*\left(\xi_0, \xi_1^{[\delta]}\right) + u^*\left(\xi_0, \xi_2^{[\delta]}\right) - u^*\left(\xi_0, \xi_3^{[\delta]}\right) - u^*\left(\xi_0, \xi_4^{[\delta]}\right) \right] d\varphi$$
$$= -\frac{\pi}{\delta} u_3(\xi_0) \quad \text{for } \xi_0 \in \gamma_2, \tag{2.6}$$

where $q_3(\varphi) := \frac{\partial u_3}{\partial r}(\delta, \varphi)$. Boundary integral equations (2.5) and (2.6) are formulated with the help of the fundamental solution for the plane Laplace equation $u^*(\xi_0, \xi) = -\ln|\xi - \xi_0|$ and with a special notation for space variables on γ_1 and γ_2 to handle the symmetry relative to the coordinate axes Ox, Oy

$\xi_1^{[\sigma]} = (\sigma, \varphi)$, $\xi_2^{[\sigma]} = (\sigma, \pi-\varphi)$, $\xi_3^{[\sigma]} = (\sigma, \pi+\varphi)$, $\xi_4^{[\sigma]} = (\sigma, 2\pi-\varphi)$ for $\sigma \in \{1, \delta\}$.

Equations (2.1), (2.5) and (2.6) are augmented by the transmission conditions on the boundaries γ_1 and γ_2, such as

$$u_1 = u_2, \quad \frac{\partial u_1}{\partial r} = \mu(h_2) \frac{\partial u_2}{\partial r} \quad \text{on } \gamma_1, \tag{2.7}$$

$$u_2 = u_3 + h_0 \delta \sin\varphi, \quad \mu(h_2) \frac{\partial u_2}{\partial r} = \frac{\partial u_3}{\partial r} + h_0 \sin\varphi \quad \text{on } \gamma_2, \tag{2.8}$$

and the symmetry conditions on the coordinate axis Ox ($\varphi = 0$) and the coordinate axis Oy ($\varphi = \pi/2$), such as

$$u_1|_{\varphi=0} = u_2|_{\varphi=0} = u_3|_{\varphi=0} = 0,$$
$$\frac{\partial u_1}{\partial \varphi}\bigg|_{\varphi=\frac{\pi}{2}} = \frac{\partial u_2}{\partial \varphi}\bigg|_{\varphi=\frac{\pi}{2}} = \frac{\partial u_3}{\partial \varphi}\bigg|_{\varphi=\frac{\pi}{2}} = 0. \tag{2.9}$$

Note that the potential $u_3(r, \varphi)$ in the formulation (2.1)–(2.9) tends to zero at the infinity due to the change of variables in the original problem statement $u_3(r, \varphi) = u_3^{original}(r, \varphi) - \mathrm{h}_0 r \sin \varphi$, where the potential $\mathrm{h}_0 r \sin \varphi$ corresponds to the applied field $(0, \mathrm{h}_0)$. The unknown functions of the mathematical model (2.1)–(2.9) are the potential function $u_2(r, \varphi) : \Omega_2 \to \mathbb{R}$ and the normal derivatives of the potential on the layer boundaries $q_1(\varphi) : [0, \pi/2] \to \mathbb{R}$ and $q_3(\varphi) : [0, \pi/2] \to \mathbb{R}$.

Due to the assumption of a uniform particle distribution in the ferrofluid layer, made in [9], the mathematical model (2.1)–(2.9) is valid only for the short-term equilibrium, when the time of the onset of the equilibrium state is much shorter than the characteristic diffusion time of concentration $\tau << \tau_{diff} \sim 40$ days, estimated for a benzene-based ferrofluid, see, e.g., in [11]. For the long-term equilibrium, $\tau \sim \tau_{diff}$. Then the diffusion of nanoparticles in ferrofluid becomes essential and the mathematical model (2.1)–(2.9) should be coupled with the mass transfer equation for nanosized ferroparticles in a ferrofluid.

When no particle interactions are assumed, the mass transfer equation for the magnetic nanoparticles in weakly concentrated ferrofluids has an explicit analytical solution in a steady-state limit for the particle concentration $C = C(h)$ as a function of the magnetic field in the ferrofluid, see, e.g., [14]. Note that the magnetic field is the position-dependent function $h = h(r, \varphi)$ and, as a consequence, the concentration function $C = C(h) = C(r, \varphi)$ also changes in space. For the problem under consideration,

$$C(h) = C_0 \frac{|\Omega_2|}{\int\limits_{\Omega_2} \psi(h) r dr d\varphi} \psi(h) \quad \text{in } \Omega_2. \tag{2.10}$$

Here $C_0 = const > 0$ corresponds to the concentration for the uniform particle distribution in the ferrofluid when no external field is applied, i.e. $C(0) = C_0$, $\psi(h) = \frac{\sinh(h)}{h}$, and the volume of the layer $|\Omega_2| = \pi(\delta^2 - 1)/4$, see Figure 1. The Langevin magnetization law with a linear dependence on the particle concentration is valid for weakly concentrated ferrofluids. See, e.g., the references in [16]. Then the relative magnetic permeability of the ferrofluid $\mu_{(1)}(h)$ in (2.2) is changed to as follows

$$\mu_{(1)}(h, C) = 1 + 3\chi_L \frac{C}{C_0} \frac{L(h)}{h} \text{ or } \mu_{(1)}(h) = 1 + \frac{3\chi_L |\Omega_2|}{\int\limits_{\Omega_2} \psi(h) r dr d\varphi} \frac{\psi(h) L(h)}{h}. \tag{2.11}$$

Mathematical model of magnetic shielding for weakly concentrated ferrofluids with non-uniform particle distribution takes form of the Equations (2.1), (2.5), (2.6) with the relative magnetic permeability $\mu_{(1)}(h)$ from (2.11) and conditions (2.7)–(2.9). Mathematical model (2.1), (2.5)–(2.9), (2.11) for weakly concentrated ferrofluids with non-uniform particle distribution is named model 1 hereinafter. By construction, model 1 takes into account magnetophoresis in the ferrofluid but neglects particle interactions. The only difference between the mathematical models for weakly concentrated ferrofluids with uniform versus non-uniform particle distribution is in the formulation of the magnetic permeability $\mu_{(1)}(h)$, that is (2.2) versus (2.11).

The dynamic mass transfer equation for the magnetic nanoparticles in concentrated ferrofluids is derived in [17]. It takes into account magnetic dipole-dipole, steric and hydrodynamic interactions between particles in magnetic fields. Under the assumptions that the layer boundaries are solid and immovable, the temperature is constant and the normal component of the particle flux over the ferrofluid boundary equals zero, the mass transfer equation in a static limit could be reformulated as an algebraic equation for the particle concentration by equating the full particle flux in the ferrofluid domain to zero, see [17],

$$\ln C + \frac{3-C}{(1-C)^3} - \frac{\partial(C^2 G(\lambda, C))}{\partial C} = \ln \psi\left(\tilde{h}_{(3)}\right) + c \quad \text{in } \Omega_2, \qquad (2.12)$$

where the effective field $\tilde{h}_{(3)}$ depends on the concentration, in contrast to (2.4):

$$\tilde{h}_{(3)} = h + \chi_L \frac{C}{C_0} L(h) + \frac{1}{16} \chi_L^2 \frac{C}{C_0} L(h) \frac{dL(h)}{dh}. \qquad (2.13)$$

Here $G(\lambda, C)$ is a given function, see [17, equation (19)], $\lambda = const > 0$ is the dipolar coupling constant, c denotes an unknown integration constant. Note that the effective field (2.13) for the Equation (2.12) can be defined for moderately concentrated ferrofluids with only the first two terms, which correspond to the magnetization law, proposed in [19],

$$\ln C + \frac{3-C}{(1-C)^3} - \frac{\partial(C^2 G(\lambda, C))}{\partial C} = \ln \psi\left(\tilde{h}_{(2)}\right) + c, \quad \text{in } \Omega_2, \qquad (2.14)$$

$$\tilde{h}_{(2)} = h + \chi_L \frac{C}{C_0} L(h).$$

The algebraic relation (2.14) was used in [10, 11] for computations of the Rosensweig instability in ferrofluids. The form of the magnetization law with concentration changes the relative magnetic permeability of the ferrofluid $\mu_{(2)}(h)$ in (2.3) and $\mu_{(3)}(h)$ in (2.4) as follows:

$$\mu_{(2)}(h, C) = 1 + 3\chi_L \frac{C}{C_0} \frac{L\left(\tilde{h}_{(2)}\right)}{h}, \qquad (2.15)$$

$$\mu_{(3)}(h, C) = 1 + 3\chi_L \frac{C}{C_0} \frac{L\left(\tilde{h}_{(3)}\right)}{h}. \qquad (2.16)$$

In addition, the condition of the particle conservation is added to the model:

$$\int_{\Omega_2} C r \, dr \, d\varphi = C_0 |\Omega_2|, \qquad (2.17)$$

where the volume fraction of magnetic particles in the carrier-liquid is fixed by the value C_0 for any applied field intensity. Based on condition (2.17), an algebraic equation will be constructed for the unknown integration constant c in (2.12) and (2.14). Mathematical model of magnetic shielding for moderately concentrated ferrofluids with non-uniform particle distribution takes

the form of the Equations (2.1), (2.5), (2.6) and (2.14) with the relative magnetic permeability $\mu_{(2)}(h, C)$ from (2.15) and the conditions (2.7)–(2.9), (2.17). Mathematical model (2.1), (2.5)–(2.9), (2.14), (2.15), (2.17) for moderately concentrated ferrofluids with non-uniform particle distribution is named model 2 hereinafter. The mathematical model of magnetic shielding for highly concentrated ferrofluids with non-uniform particle distribution takes the form of the Equations (2.1), (2.5), (2.6) and (2.12) with relative magnetic permeability $\mu_{(3)}(h, C)$ from (2.16) and conditions (2.7)–(2.9), (2.17). Mathematical model (2.1), (2.5)–(2.9), (2.12), (2.16), (2.17) for highly concentrated ferrofluids with non-uniform particle distribution is named model 3 hereinafter. By construction, model 2 and model 3 take into account magnetophoresis and the particle interaction in the ferrofluid. The unknown functions of model 2 and model 3, in contrast to model 1, are not only the potential function $u_2(r, \varphi)$ and the normal derivatives of the potential on the layer boundaries $q_1(\varphi)$ and $q_3(\varphi)$ but also the concentration function $C(r, \varphi) : \Omega_2 \to \mathbb{R}$ inside the ferrofluid.

The constructed mathematical models are based on different levels of theory for describing magnetization laws for ferrofluids at low, medium and high particle concentrations. Refer to [8, 16, 19]. They are based on the theoretical model in [17] for describing magnetophoresis in ferrofluids with interacting particles. The accuracy of theoretical models in [8, 16, 17, 19] is estimated by comparing with experimental data and numerical results of molecular dynamics modelling.

Three mathematical models will be compared to each other, based on results of computations, under the assumption that the model 3, by construction, is more accurate for computations with ferrofluids of any kind of concentration: weakly, moderately or highly concentrated ones. Model 3 is the most complicated one in the mathematical formulation in comparison with model 1 and model 2.

3 Computational algorithm

The computations were carried out in the polar coordinate system $Or\varphi$ on a uniform rectangular mesh in the domain $[1, \delta] \times [0, \pi/2]$ with the mesh nodes

$$\left\{ (r_i, \varphi_j) \,:\, r_i = i\Delta r, \varphi_j = j\Delta\varphi, \quad i = \overline{0, N_r}, j = \overline{0, N_\varphi} \right\}$$

and the corresponding rectangular mesh elements

$$\left\{ T_{ij} = [r_i, r_{i+1}] \times [\varphi_j, \varphi_{j+1}] \,:\, i = \overline{0, N_r - 1}, j = \overline{0, N_\varphi - 1} \right\},$$

where $\Delta r = (\delta - 1)/N_r$, $\Delta\varphi = \pi/2/N_\varphi$, see Figure 2. We choose $N_r = 10$ and $N_\varphi = 100$ for $\delta \in [1.01, 2]$, analogous to the previous computations in [9,15]. The test calculations on a finer mesh with twice the number of partitions ($N_r = 20$, $N_\varphi = 200$) did not reveal any significant changes in the solution. Namely, the potential function and the concentration function differ on both meshes in the fourth significant digit.

The computational process is organized in the form of an iterative algorithm, where the magnetostatics subproblem for the known concentration and
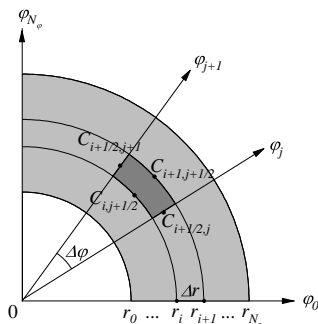
Figure 2. Schematic representation of the mesh for computations in the layer Ω_2.

the concentration subproblem for the known potential are solved independently at every iteration. Two subproblems are successively solved up to a convergence relative to the unknown potential and concentration functions. Note that the iterative algorithm for model 1 reduces to one iteration at which only the magnetostatics subproblem should be solved, due to the known exact solution (2.10) for the concentration subproblem.

Numerical solution of the magnetostatics subproblem (2.1), (2.5)–(2.9) for the concentration dependent relative magnetic permeabilities (2.11), (2.15), (2.16) in the context of models 1–3, respectively, under the assumption that the concentration function is known, is realized by means of the coupled method of finite differences and boundary elements. Refer to [9, 15] for details. The unknown values for the potential function $u_2(r, \varphi)$ are defined at the mesh nodes, whereas the unknown values for the normal derivatives of the potential $q_1(\varphi)$ and $q_3(\varphi)$ are defined at the corresponding nodes on interfaces $\{(1, \varphi_j)\}$ and $\{(\delta, \varphi_j)\}$, $j = \overline{0, N_\varphi}$.

The concentration subproblem is defined in the form of the explicit relation (2.10) for model 1, in the form of the Equations (2.12) and (2.17) for model 2 and in the form of the Equations (2.14) and (2.17) for model 3. The algebraic Equations (2.12) and (2.14) are valid at any point of the ferrofluid domain Ω_2:

$$\ln C + R(C) - \ln \psi\big(\tilde{h}_{(i)}\big) = c, \tag{3.1}$$

where $R(C) := \frac{3-C}{(1-C)^3} - \frac{\partial(C^2 G(\lambda, C))}{\partial C}$, $i = 2$ or 3 for corresponding models. We reformulate (3.1) by taking the exponent of both sides of the equation:

$$\Phi(h, C) := C e^{R(C)} \tilde{h}_{(i)}\,(h, C)/\sinh\big(\tilde{h}_{(i)}\,(h, C)\big) = c, \tag{3.2}$$

where the constant c in (3.1) and (3.2) has different values. Let us assume that a spacial configuration of the magnetic field $h(r, \varphi)$ is given at the middle points of the mesh lines from a solution of the magnetostatics subproblem

$$h_{i+1/2,j} = h(r_{i+1/2}, \varphi_j), \quad i = \overline{0, N_r - 1}, j = \overline{0, N_\varphi},$$
$$h_{i,j+1/2} = h(r_i, \varphi_{j+1/2}), \quad i = \overline{0, N_r}, j = \overline{0, N_\varphi - 1},$$

where $r_{i+1/2} = (r_i + r_{i+1})/2$, $\varphi_{i+1/2} = (\varphi_i + \varphi_{i+1})/2$. We construct algebraic equations for the unknown concentration values $C_{i+1/2,j}$ and $C_{i,j+1/2}$ at the middle points of the mesh lines, see Figure 2, by satisfying Equation (3.2) at the following corresponding points:

$$\Phi(h_{i+1/2,j}, C_{i+1/2,j}) - c = 0, \quad i = \overline{0, N_r - 1}, j = \overline{0, N_\varphi}, \tag{3.3}$$

$$\Phi(h_{i,j+1/2}, C_{i,j+1/2}) - c = 0, \quad i = \overline{0, N_r}, j = \overline{0, N_\varphi - 1}. \tag{3.4}$$

Moreover, an additional algebraic equation is derived from the conservation condition for the concentration (2.17) by applying the quadrature formula at the centers of the element sides. Namely,

$$\sum_{T_{ij}} \frac{\omega_{ij}}{4} \left(C_{i,j+1/2} + C_{i+1/2,j} + C_{i+1,j+1/2} + C_{i+1/2,j+1} \right) \approx C_0 \sum_{T_{ij}} \omega_{ij},$$

where the summation is taken over all mesh elements. The volume of the mesh element T_{ij} equals $\omega_{ij} = \int_{T_{ij}} r \, dr \, d\varphi = r_{i+1/2} \Delta r \Delta \varphi$. We reformulate the last relation as an equation in the following form:

$$\sum_{i=0}^{N_r-1} \sum_{j=0}^{N_\varphi} \frac{\omega_{ij} + \omega_{i,j-1}}{4} (C_{i+1/2,j} - C_0)$$

$$+ \sum_{i=0}^{N_r} \sum_{j=0}^{N_\varphi-1} \frac{\omega_{ij} + \omega_{i-1,j}}{4} \left(C_{i,j+1/2} - C_0 \right) = 0, \tag{3.5}$$

where we set $\omega_{ij} = 0$ for $i \in \{-1, N_r\}$ or $j \in \{-1, N_\varphi\}$. As a result, the concentration subproblem for model 2 and model 3 is formulated as a system of nonlinear algebraic equations (3.3)–(3.5) for the unknown concentration values $\{C_{i+1/2,j}, i = \overline{0, N_r - 1}, j = \overline{0, N_\varphi}\}$, $\{C_{i,j+1/2}, i = \overline{0, N_r}, j = \overline{0, N_\varphi - 1}\}$ and the unknown constant c. The system of algebraic equations (3.3)–(3.5) is solved by Newton's method, which, in a general case of a system $\mathbf{F}(\mathbf{x}) = \mathbf{0}$, is an iterative process of the form

$$\mathbf{F}'(\mathbf{x}^k) \left(\mathbf{x}^{k+1} - \mathbf{x}^k \right) = -\mathbf{F}(\mathbf{x}^k), \quad k = 0, 1, 2, \dots. \tag{3.6}$$

Here $\mathbf{F}(\mathbf{x}) = (f_1(\mathbf{x}), \dots, f_n(\mathbf{x}))$, $\mathbf{x}^k \in \mathbb{R}^n$, $\mathbf{F}'(\mathbf{x}) = \left(\frac{\partial f_i(\mathbf{x})}{\partial x_j} \right)_{i,j=\overline{1,n}}$, and the initial value $\mathbf{x}^0 \in \mathbb{R}^n$ is given. Let us introduce notations

$$\Phi_{ij}^k = \Phi\left(h_{ij}, C_{ij}^k \right), \quad \frac{\partial \Phi_{ij}^k}{\partial C} = \frac{\partial \Phi}{\partial C} \left(h_{ij}, C_{ij}^k \right).$$

Then the equations of the Newton system (3.6), corresponding to the algebraic Equations (3.3), take the form

$$\frac{\partial \Phi_{i+1/2,j}^k}{\partial C} \left(C_{i+1/2,j}^{k+1} - C_{i+1/2,j}^k \right) - (c^{k+1} - c^k) = - \left(\Phi_{i+1/2,j}^k - c^k \right)$$

or, alternatively, they can be rewritten as

$$C_{i+1/2,j}^{k+1} = C_{i+1/2,j}^k - \frac{\Phi_{i+1/2,j}^k - c^{k+1}}{\partial \Phi_{i+1/2,j}^k / \partial C}, \quad i = \overline{0, N_r - 1}, j = \overline{0, N_\varphi}. \tag{3.7}$$

The equations of the Newton system (3.6), corresponding to the algebraic Equations (3.4), take the form

$$\frac{\partial \Phi_{i,j+1/2}^k}{\partial C}\left(C_{i,j+1/2}^{k+1} - C_{i,j+1/2}^k\right) - \left(c^{k+1} - c^k\right) = -\left(\Phi_{i,j+1/2}^k - c^k\right)$$

or alternatively they can be rewritten as

$$C_{i,j+1/2}^{k+1} = C_{i,j+1/2}^k - \frac{\Phi_{i,j+1/2}^k - c^{k+1}}{\partial \Phi_{i,j+1/2}^k/\partial C}, \quad i = \overline{0, N_r}, j = \overline{0, N_\varphi - 1}. \tag{3.8}$$

Let us substitute the expressions for $C_{i+1/2,j}^{k+1}$ and $C_{i,j+1/2}^{k+1}$ from (3.7) and (3.8), respectively, into the equation of the Newton system, corresponding to the Equation (3.5),

$$\sum_{i=0}^{N_r-1}\sum_{j=0}^{N_\varphi} \frac{\omega_{ij} + \omega_{i,j-1}}{4} \frac{c^{k+1} - \Phi_{i+1/2,j}^k}{\frac{\partial \Phi_{i+1/2,j}^k}{\partial C}} + \sum_{i=0}^{N_r}\sum_{j=0}^{N_\varphi-1} \frac{\omega_{ij} + \omega_{i-1,j}}{4} \frac{c^{k+1} - \Phi_{i,j+1/2}^k}{\frac{\partial \Phi_{i,j+1/2}^k}{\partial C}}$$

$$= -\sum_{i=0}^{N_r-1}\sum_{j=0}^{N_\varphi} \frac{\omega_{ij}+\omega_{i,j-1}}{4}\left(C_{i+1/2,j}^k - C_0\right) - \sum_{i=0}^{N_r}\sum_{j=0}^{N_\varphi-1} \frac{\omega_{ij}+\omega_{i-1,j}}{4}\left(C_{i,j+1/2}^k - C_0\right).$$

According to the last relation, the value of the unknown constant c^{k+1} could be expressed explicitly through the values at the k-th iteration of the Newton method

$$c^{k+1} = \left(\sum_{i=0}^{N_r-1}\sum_{j=0}^{N_\varphi} \frac{\omega_{ij} + \omega_{i,j-1}}{4}\left(\frac{\Phi_{i+1/2,j}^k}{\partial \Phi_{i+1/2,j}^k/\partial C} - C_{i+1/2,j}^k + C_0\right)\right.$$

$$+ \sum_{i=0}^{N_r}\sum_{j=0}^{N_\varphi-1} \frac{\omega_{ij} + \omega_{i-1,j}}{4}\left(\frac{\Phi_{i,j+1/2}^k}{\partial \Phi_{i,j+1/2}^k/\partial C} - C_{i,j+1/2}^k + C_0\right)\right)$$

$$\left/\left(\sum_{i=0}^{N_r-1}\sum_{j=0}^{N_\varphi} \frac{\omega_{ij} + \omega_{i,j-1}}{4}\left(\frac{\partial \Phi_{i+1/2,j}^k}{\partial C}\right)^{-1}\right.\right.$$

$$+ \left.\left.\sum_{i=0}^{N_r}\sum_{j=0}^{N_\varphi-1} \frac{\omega_{ij} + \omega_{i-1,j}}{4}\left(\frac{\partial \Phi_{i,j+1/2}^k}{\partial C}\right)^{-1}\right). \tag{3.9}$$

Due to the structure of the Newton system (3.7)–(3.9), computations at each iteration are reduced to successive calculations of the unknown quantities. Namely, we first compute c^{k+1} by (3.9), then $C_{i+1/2,j}^{k+1}$ and $C_{i,j+1/2}^{k+1}$ by (3.7) and (3.8), respectively, for the known value of c^{k+1}.

The Newton method requires up to 10 iterations to converge until the norms of the relative errors $\|C^{k+1} - C^k\|_\infty/C_0$ and $|c^{k+1} - c^k|/|c^k|$ become less than 10^{-7}. Initial values for the Newton iterations are defined as $C_{ij}^0 = C_0$ and $c^0 = C_0 e^{R(C_0)}$ from (3.2). These correspond to the applied field intensity equaled to zero and, consequently, $h = 0$ inside the ferrofluid domain.

Note that the expression for the unknown constant c^{k+1} is incorrectly written in [10] and should be modified as

$$c^{k+1} = \sum_{i=1}^{M} \omega_i \left(\frac{\Phi\left(C_i^k, H_i\right)}{\frac{\partial \Phi}{\partial C}\left(C_i^k, H_i\right)} - C_i^k + C_0 \right) \Big/ \sum_{i=1}^{M} \frac{\omega_i}{\frac{\partial \Phi}{\partial C}\left(C_i^k, H_i\right)},$$

following the notations in [10].

4 Numerical results

The dimensionless parameters of the problem under consideration are the applied field intensity h_0, the outer radius of the layer δ, the Langevin susceptibility of ferrofluid χ_L and the mean particle concentration of ferrofluid C_0.

For the test computations, three different ferrofluids are considered, named as MF1, MF2 and MF3, with the following characteristics: the saturation magnetization M_s, the magnetic phase concentration ϕ_m, the Langevin susceptibility χ_L and the mean particle concentration C_0, taken from [21, Table II] for monodisperse ferrofluids at $T = 295$ K. Namely,

for MF1: $M_s = 25$ kA/m, $\phi_m = 0.052083$, $\chi_L = 1.748484$, $C_0 = 0.111042$,

for MF2: $M_s = 50$ kA/m, $\phi_m = 0.104167$, $\chi_L = 3.496968$, $C_0 = 0.222084$,

for MF3: $M_s = 75$ kA/m, $\phi_m = 0.156250$, $\chi_L = 5.245452$, $C_0 = 0.333126$.

The ferrofluids MF1, MF2, MF3 correspond to classes of weakly, moderately and highly concentrated ferrofluids, respectively. The dipolar coupling constant is defined by the relation $\lambda = \chi_L / (8C_0)$, see e.g. [18], and it is equal to the same value $\lambda \approx 1.96827$ for the ferrofluids under consideration. As a result, the left-hand sides of the algebraic equations for the concentration (2.12) and (2.14) are the same for ferrofluids MF1, MF2 and MF3, making computations easier.

The cylindrical geometry of the ferrofluid layer results in a significant steady-state redistribution of ferroparticles inside the layer due to the diffusion process of nanoparticles. Refer to Figure 3.

The particle concentration takes the maximum value near the Ox-axis. Moving counterclockwise for the polar angle from 0 to $\pi/2$, the concentration monotonically decreases to the minimum value near the Oy-axis. Refer to the isolines structure in Figure 3a and the concentration profile over the center line of the ferrofluid domain at $r = (1 + \delta)/2$ in Figure 3b. In particular, for the ferrofluid MF3 at $h_0 = 10$ the maximum value is at about $1.3C_0$ and the minimum value is about $0.5C_0$. Refer to Figure 3a. Ferrofluids MF1, MF2, MF3 have different values of the mean particle concentration C_0 resulting in a different quantitative particle redistribution inside the ferrofluid layer for the same applied field h_0. Refer to Figure 3b. Note that the magnetic field intensity h inside the ferrofluid has the same qualitative behavior as the concentration shown in Figure 3. This is due to the algebraic relationship between C and h, which has an explicit form (2.10) for model 1 and implicit ones (2.14) and (2.12) for model 2 and model 3, respectively.
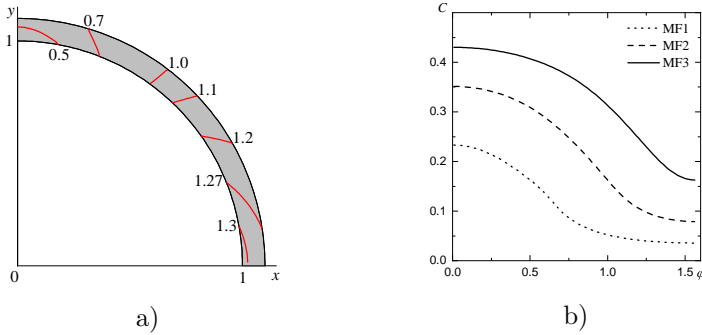
Figure 3. a) Isolines of the dimensionless concentration C/C_0 for the ferrofluid MF3. b) Dependence of the dimensional concentration C versus the polar angle on the center line of the ferrofluid domain at $r = (1 + \delta)/2$. Computations are made for model 3 at the dimensionless applied magnetic field intensity $h_0 = 10$ and at the dimensionless outer radius of the layer $\delta = 1.1$.

A physical explanation of the fact that the concentration near the Ox-axis is larger than near the Oy-axis, see Figure 3a, is due to the external magnetic field orientation along the y-direction and the transmission conditions (2.7) and (2.8) on the layer boundaries γ_1 and γ_2. The tangential component of the external magnetic field equals zero at the top point ($x = 0$, $y = \delta$). Therefore $h_2 = h_3\mu$, but at the right point ($x = \delta$, $y = 0$) the normal component of the external field equals zero. Hence $h_2 = h_3$. The values of h_3 at both points are comparable to the field intensity at the infinity. Therefore, h_2 at the right point is larger than at the top point for $\mu > 1$. As a consequence of a monotone dependence between C and h_2, the concentration at the right point is larger than at the top point.

The results of computations, presented in Figure 3, are made for model 3. Analogous computations for model 1 show the maximum relative deviation of about 50% from the results of model 3 for the concentration values at some regions even for the weakly concentrated ferrofluid MF1. We conclude that model 1 can not be used for the problem under consideration to get quantitatively valuable numerical results for MF1, MF2 and MF3 in the whole range of field intensities. Computations for Figure 3 made in the context of model 2 demonstrate the maximum relative deviation of about 0.2% from the results of model 3 for concentration values obtained for ferrofluids MF1, MF2 and MF3.

A quantitative measure of the effectiveness of a shield is defined by the shielding effectiveness factor K_{ef}, which estimates the decay factor of the applied magnetic field intensity after its transmission into the shielded region Ω_1. The shielding effectiveness factor is computed as the ratio of the magnitude of the applied field h_0 to the magnitude of the transmitted magnetic field h_1 at the observation point $r = 0$, according to the following formula:

$$K_{\mathrm{ef}} = \frac{h_0}{h_1(0, \varphi)} = h_0 / \left| \lim_{r \to 0} \frac{\partial u_1(r, \pi/2)}{\partial r} \right|.$$

See [9] for the details.

Figure 4a shows the effect of the particle redistribution inside the ferrofluid layer on the shielding effectiveness factor for different intensities of the applied magnetic field h_0. Namely, the shielding effectiveness factor K_{ef} is computed under the assumption of uniform particle distribution $C = C_0$. It is compared with the shielding effectiveness factor K_{ef}^{diff} computed in the context of the model 3 taking the particles diffusion into account. The relative error $\left(K_{ef}^{diff} - K_{ef}\right)/K_{ef}$ demonstrates that the diffusion has negligible influence (less than 1%) on the shielding factor in weak magnetic fields ($h_0 < 1$) and strong fields ($h_0 > 20$). Refer to Figure 4a. Due to the diffusion process, the highest increase of the shielding is achieved for the moderate field intensities of about $h_0 = 3$, where the relative error takes the maximum value at around 3% for the outer radius of the layer $\delta = 1.1$. Refer to Figure 4a. Similar qualitative behavior is presented for three ferrofluids under consideration, whereas the moderately concentrated ferrofluid MF2 shows the strongest increase of the shielding effectiveness factor K_{ef}^{diff}, compared with K_{ef}.
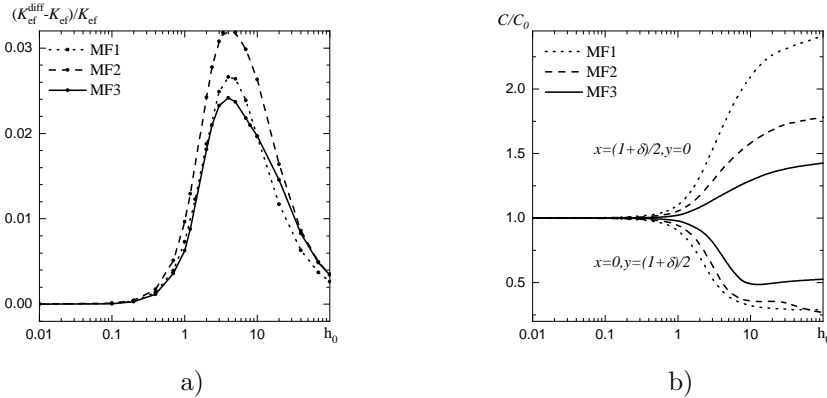
Figure 4. a) Dependence of the relative error $\left(K_{ef}^{diff} - K_{ef}\right)/K_{ef}$ for the shielding effectiveness factor, computed as K_{ef}^{diff} for a non-uniform particle distribution and as K_{ef} for a uniform one, versus the dimensionless applied magnetic-field intensity h_0.
b) Dependence of the dimensionless concentration C/C_0 versus the dimensionless applied magnetic-field intensity h_0 at the two control points $x = (1 + \delta)/2, y = 0$ and $x = 0, y = (1 + \delta)/2$ on the center line of the ferrofluid domain at $r = (1 + \delta)/2$. Computations are made for model 3 at the dimensionless outer radius of the layer $\delta = 1.1$.

Despite the fact that the effect of the diffusion on the shielding effectiveness factor is not very pronounced at the outer radius of the layer $\delta = 1.1$, see Figure 4a, the steady-state particle redistribution inside the ferrofluid layer is quite substantial. We define two control points on the center line of the ferrofluid domain at $r = (1 + \delta)/2$ to monitor the behavior of the concentration. Figure 4b shows a monotone change of the concentration with increasing magnetic field intensity h_0, applied externally. Namely, we observe a monotone increase of the concentration at the control point on the Ox-axis, whereas we see a monotone decrease of the concentration at the second control point on the Oy-axis. The strongest particle redistribution is shown for the weakly concentrated ferrofluid MF1 with the maximum concentration of about $2.4C_0$ and

the minimum value $0.3C_0$ for strong magnetic field of the intensity $h_0 = 100$. Moreover, Figure 4b shows that particles remain nearly uniformly distributed in weak fields for $h_0 < 1$ resulting in negligible influence of diffusion on the shielding factor values. Refer to Figure 4a.

Computations for Figure 4 are made in the context of model 3. Analogous computations performed for model 2 demonstrate the maximum relative deviation of about 3% from the results of model 3 for the shielding effectiveness factors K_{ef} and $K_{\mathrm{ef}}^{\mathrm{diff}}$ in the whole range of field intensities $h_0 \in [0.01, 100]$, obtained for three ferrofluids under consideration. The maximum deviation for the compared values corresponds to the highly concentrated ferrofluid MF3, whereas the deviation is about 0.1% for the weakly concentrated ferrofluid MF1 and about 1% for the moderately concentrated ferrofluid MF2. We conclude that model 2, as a simpler version of model 3 in the mathematical formulation, can be used for the problem under consideration to obtain quantitatively valuable numerical results for ferrofluids MF1, MF2 and MF3 in the whole range of field intensities.
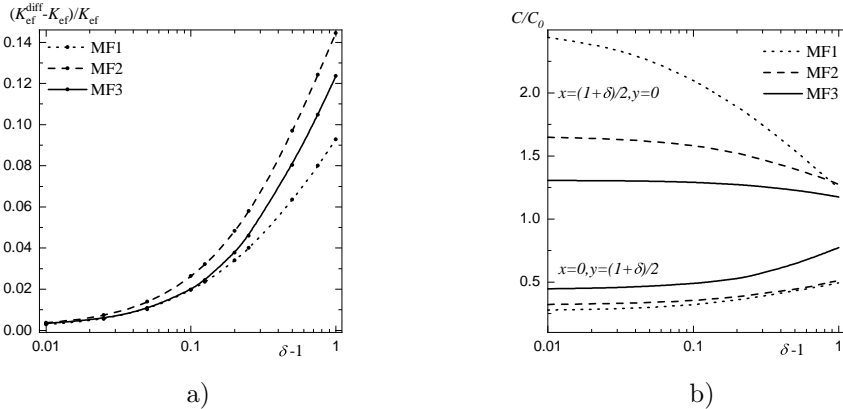
Figure 5. a) Dependence of the relative error $\left(K_{\mathrm{ef}}^{\mathrm{diff}} - K_{\mathrm{ef}} \right) / K_{\mathrm{ef}}$ for the shielding effectiveness factor, computed as $K_{\mathrm{ef}}^{\mathrm{diff}}$ for a non-uniform particle distribution and as K_{ef} for a uniform one, versus the dimensionless layer thickness $\delta - 1$. b) Dependence of the dimensionless concentration C/C_0 versus the dimensionless layer thickness $\delta - 1$ at the two control points $x = (1 + \delta)/2, y = 0$ and $x = 0, y = (1 + \delta)/2$ on the center line of the ferrofluid domain at $r = (1 + \delta)/2$. Computations are made for model 3 at the dimensionless applied magnetic-field intensity $h_0 = 10$.

Figure 5a shows the effect of the diffusion on the shielding effectiveness factor for various values of the layer thickness $\delta - 1$. The shielding effectiveness factor K_{ef}, computed for the uniform particle distribution $C = const$, is compared to the shielding effectiveness factor $K_{\mathrm{ef}}^{\mathrm{diff}}$, computed for the non-uniform particle distribution $C = C(h)$ in the context of the model 3. The relative error $\left(K_{\mathrm{ef}}^{\mathrm{diff}} - K_{\mathrm{ef}} \right) / K_{\mathrm{ef}}$ demonstrates that the diffusion leads to a monotone increase of the shielding effectiveness factor up to the value close to 10%, with increasing outer radius of the layer $\delta \in [1.01, 2]$ at the moderate field intensity $h_0 = 10$. Refer to Figure 5a. All three ferrofluids under consideration show

a similar monotone behavior in Figure 5a. The moderately concentrated ferrofluid MF2 demonstrates the strongest increase of the shielding effectiveness factor, due to the diffusion, compared to the weakly concentrated ferrofluid MF1 and the highly concentrated ferrofluid MF3. This fact is supported by the numerical results in Figure 4a and Figure 5a. The values of the shielding effectiveness factor are higher for more concentrated ferrofluids. Refer to [9]. However, the relative quantity $\left(K_{\text{ef}}^{\text{diff}} - K_{\text{ef}}\right)/K_{\text{ef}}$, presented in Figure 4a and Figure 5a, may lose this qualitative effect. For example, at $h_0 = 3$ the factor values ($K_{\text{ef}} = 1.12$, $K_{\text{ef}}^{\text{diff}} = 1.16$) for the moderately concentrated ferrofluid MF2 are smaller than $K_{\text{ef}} = 1.23$, $K_{\text{ef}}^{\text{diff}} = 1.26$ for the highly concentrated ferrofluid MF3. However, the relative quantity $\left(K_{\text{ef}}^{\text{diff}} - K_{\text{ef}}\right)/K_{\text{ef}} = 0.03$ for MF2 is higher than $\left(K_{\text{ef}}^{\text{diff}} - K_{\text{ef}}\right)/K_{\text{ef}} = 0.02$ for MF3.

Figure 5b shows that the steady-state particle redistribution is stronger inside thin layers than inside thick ones with a tendency to reach uniform distribution with increasing layer thickness $\delta - 1$. In particular, the strongest particle redistribution is shown for the weakly concentrated ferrofluid MF1 with the maximum concentration of about $2.4C_0$ and the minimum value $0.3C_0$ for thin layer with $\delta = 1.01$ at $h_0 = 10$. A monotone change of the concentration with increasing layer thickness $\delta - 1$ is shown in Figure 5b with a monotone increase of the concentration at the control point on the Ox-axis for $r = (1 + \delta)/2$ and a monotone decrease at the second control point on the Oy-axis for $r = (1 + \delta)/2$.

The computation results, presented in Figure 5, are made in the context of model 3. Analogous computations, performed for model 2, demonstrate the maximum relative deviation of about 0.05% from the results of model 3 for the shielding effectiveness factors K_{ef} and $K_{\text{ef}}^{\text{diff}}$ in the whole range of $\delta \in [1.01, 2]$, obtained for three ferrofluids under consideration.

Based on computation results of the three models, presented in Figure 3–Figure 5, one may notice the maximum relative deviation between model 1 and model 3 is about 50% in Figure 3, and the maximum relative deviation between model 2 and model 3 is about 3% in Figure 4. Note that the relative accuracies of the numerical results correlate with the relative deviations in the values of the initial susceptibilities corresponding to three models under consideration. The known expressions for the initial susceptibilities are $\chi_{(1)} = \chi_L$, $\chi_{(2)} = \chi_L(1 + \chi_L/3)$ and $\chi_{(3)} = \chi_L(1 + \chi_L/3 + \chi_L^2/144)$, see e.g. [21]. Relative deviations between $\chi_{(1)}$ and $\chi_{(3)}$ range from 38% to 66%, whereas relative deviation between $\chi_{(2)}$ and $\chi_{(3)}$ range from 1.3% to 6.5% for MF1, MF2 and MF3. These numbers are of the same order of magnitude as those found in numerical computations. We conclude that model 1 cannot be used for the problem under consideration to get quantitatively valuable numerical results for MF1, MF2 and MF3. We also conclude that model 2, as a simpler version of model 3 in the mathematical formulation, suits well for the modelling in the whole range of the applied field intensities h_0 and of the layer thicknesses for MF1, MF2 and MF3.

5 Conclusions

Three mathematical models are constructed and compared under the assumption that model 3, by construction, is more accurate for computations with weakly, moderately and highly concentrated ferrofluids. Model 1 can not be used for the problem under consideration to get quantitatively valuable numerical results for any type of ferrofluids. Model 2, as a simpler version of model 3 in the mathematical formulation, suits well for the numerical modelling of the problem under consideration in the wide range of the applied field intensities h_0 and of the ferrofluid layer thicknesses $\delta - 1$.

The shielding effectiveness factor is mostly influenced by the particle redistribution inside the ferrofluid layer at moderate intensities of the applied field h_0 leading to an increase of the shielding effectiveness factor $K_{\text{ef}}^{\text{diff}}$ of up to 10%, by comparing with the results of computations without diffusion. Refer to Figure 4a and Figure 5a. The shielding properties of the ferrofluid layer is not improved by diffusion at weak and strong intensities of the applied field h_0. Refer to Figure 4a. Most likely, the diffusion of magnetic particles will lead to a stronger increase of the shielding effectiveness factor in non-uniform external magnetic fields.

The weakly concentrated ferrofluid (magnetic phase equals 0.05) shows the strongest particle redistribution inside the ferofluid layer compared to concentration profiles for the moderately and the highly concentrated ferrofluids. Refer to Figure 4b and Figure 5b. However, due to diffusion, the increase of the shielding effectiveness factor $K_{\text{ef}}^{\text{diff}}$ is higher for the moderately concentrated ferrofluid (magnetic phase equals 0.1) than for the weakly and the highly concentrated ferrofluid. Refer to Figure 4a and Figure 5a.

Acknowledgements

References

[1] B.M. Berkovsky and V. Bashtovoi. *Magnetic fluids and applications handbook.* Begell House Inc. Publ., New York, 1996.

[2] B.M. Berkovsky, V.F Medvedev and M.S. Krakov. *Magnetic fluids: engineering applications.* Oxford University Press, Oxford, 1993.

[3] A. Cebers, E. Blum and M.M. Maiorov. *Magnetic fluids.* Walter de Gruyter, Berlin, 1997.

[4] S. Celozzi, R. Araneo and G. Lovat. *Electromagnetic Shielding.* John Wiley & Sons, 2008. https://doi.org/10.1002/9780470268483.

[5] B. Dolník, M. Rajňák, R. Cimbala, I. Kolcunová, J. Kurimský, J. Balogh, J. Džmura, J. Petráš, P. Kopčanský, M. Timko, J. Briančin and M. Fabián. The response of a magnetic fluid to radio frequency electromagnetic field. *Acta Physica Polonica A*, **131**(4):946–948, 2017. https://doi.org/10.12693/APhysPolA.131.946.

[6] B. Dolník, M. Rajňák, R. Cimbala, I. Kolcunová, J. Kurimský, J. Džmura, J. Petráš, J. Zbojovský, M. Kosterec, P. Kopčanský and M. Timko. The shielding effectiveness of a magnetic fluid in radio frequency range. *Acta Physica Polonica A*, **133**(3):585–587, 2018. https://doi.org/10.12693/APhysPolA.133.585.

[7] V. Glyva, N. Kasatkina, V. Nazarenko, N. Burdeina, N. Karaieva, L. Levchenko, O. Panova, O. Tykhenko, B. Khalmuradov and O. Khodakovskyy. Development and study of protective properties of the composite materials for shielding the electromagnetic fields of a wide frequency range. *Eastern-European Journal of Enterprise Technologies*, **2**(12):40–47, 2020. https://doi.org/10.15587/1729-4061.2020.201330.

[8] A.O. Ivanov and O.B. Kuznetsova. Magnetic properties of dense ferrofluids: An influence of interparticle correlations. *Physical Review E*, **64**:041405, 2001. https://doi.org/10.1103/PhysRevE.64.041405.

[9] O. Lavrova, V. Polevikov and S. Polevikov. Numerical modelling of magnetic shielding by a cylindrical ferrofluid layer. *Math. Model. Anal.*, **24**(2):155–170, 2019. https://doi.org/10.3846/mma.2019.011.

[10] O. Lavrova, V. Polevikov and L. Tobiska. Numerical study of diffusion of interacting particles in a magnetic fluid layer. In P. Miidla(Ed.), *Numerical Modelling*, pp. 183–202. IntechOpen, 2012. https://doi.org/10.5772/36636.

[11] O. Lavrova, V. Polevikov and L. Tobiska. Modeling and simulation of magnetic particles diffusion in a ferrofluid layer. *Magnetohydrodynamics*, **52**(4):439–452, 2016. https://doi.org/10.22364/mhd.52.4.1.

[12] M. Mishra, A.P. Singh, B.P. Singh, V.N. Singh and S.K. Dhawan. Conducting ferrofluid: a high-performance microwave shielding material. *J. Mater. Chem. A*, **2**(32):13159–13168, 2014. https://doi.org/10.1039/C4TA01681E.

[13] H. Mohseni. Dynamic magnetic shielding and beamforming using ferrofluid for compact magnetoencephalography (meg). *US Patent US20200088811A1*, 2019.

[14] V. Polevikov and L. Tobiska. On the solution of the steady-state diffusion problem for ferromagnetic particles in a magnetic fluid. *Math. Model. Anal.*, **13**(2):233–240, 2008.

[15] V.K. Polevikov and B.T. Erofeenko. Numerical modelling of the interaction of a magnetic field with a cylindrical magnetic-fluid layer. *Informatika*, **2**(54):5–13, 2017. (in Russian)

[16] A.F. Pshenichnikov. Equilibrium magnetization of concentrated ferrocolloids. *J. Magn. Magn. Mater.*, **145**(3):319–326, 1995. https://doi.org/10.1016/0304-8853(94)01632-1.

[17] A.F. Pshenichnikov, E.A Elfimova and A.O. Ivanov. Magnetophoresis, sedimentation, and diffusion of particles in concentrated magnetic fluids. *J. Chem. Phys.*, **134**:184508, 2011. https://doi.org/10.1063/1.3586806.

[18] A.F. Pshenichnikov and A.V. Lebedev. Magnetic susceptibility of concentrated ferrocolloids. *Colloid J.*, **67**:189–200, 2005. https://doi.org/10.1007/s10595-005-0080-x.

[19] A.F. Pshenichnikov, V.V. Mekhonoshin and A.V. Lebedev. Magneto-granu-lometric analysis of concentrated ferrocolloids. *J. Magn. Magn. Mater.*, **161**:94–102, 1996. https://doi.org/10.1016/S0304-8853(96)00067-4.

[20] R.E. Rosensweig. *Ferrohydrodynamics.* Dover Pubns, New York, 1998.

[21] A.Y. Solovyova, E.A. Elfimova, A.O. Ivanov and P.J. Camp. Modi-fied mean-field theory of the magnetic properties of concentrated, high-susceptibility, polydisperse ferrofluids. *Physical Review E*, **96**:052609, 2017. https://doi.org/10.1103/PhysRevE.96.052609.